JASTT

Point Cloud Approach For Modelling The Lost Volume of The Fillaboa Bridge Cutwater

Jesús Balado*and Ana Sánchez-Rodríguez

Universidade de Vigo, CINTECX, GeoTECH group. 36310 Vigo, España (jbalado, anasanchez)@uvigo.es
*Correspondence: jbalado@uvigo.es

Abstract

The digitization of heritage is being rapidly realised in many parts of the world, thanks to LiDAR technology. In addition to the simple digital preservation of heritage, 3D acquisition makes it possible to monitor the structural condition and assess possible damage. This paper presents a method for modelling the lost volume of a heritage bridge. The selected case study is the Fillaboa bridge in Salvaterra de Miño, Spain, which has two cutwaters with the same cutting angle, one of which is damaged and has a stone loss. The bridge was acquired with a Terrestrial Laser Scanner. The method consists of the following processes. First, the walls of the whole cutwater are segmented and aligned by the Iterative Closest Point algorithm over the damaged cutwater. Second, the distance between the two point clouds is calculated, and the damaged area is delimited in both point clouds. And third, the alpha-shape algorithm is applied to model the point cloud of the damaged area on a polygon. By searching for the optimal alpha radius, the polygon that best fits the damaged volume is generated. The proposed method also allows digital reconstruction of the damaged area, although it is sensitive to acquisition problems, which require manual interventions in the processing. The accuracy of the method is mainly dependent on the acquired point cloud registration (with an RMS error of 60mm) and the ICP registration error (31mm). Its use is limited to the existence of two geometries that allow superposition: one in good condition and one damaged to compare.

I. INTRODUCTION

LiDAR technology has now become established for the rapid heritage digitization [1–3]. Several factors have led to this development. The reduction in the price of laser scanners due to their integration into the autonomous vehicles [4]. The high accuracy and speed of acquisition [5]. The specialisation of LiDAR equipment, being installed on a multitude of platforms [6,7]. The development of new automatic point cloud processing techniques with Artificial Intelligence [8,9]. And the consideration of the point cloud as a model, without the need for transformation to other standards [10].

The digitisation of heritage has shown several advantages for both experts and tourists. Multi-temporal acquisitions are useful for studying deterioration [11] by comparing digital models over time. Archaeological sites can be digitally reconstructed without making aggressive interventions on the original site [12]. Experts and tourists can access heritage sites and museum pieces from other parts of the world without travelling and even feel an immersive experience through Virtual Reality [13].

Despite the widespread use of LiDAR in heritage digitisation, there are still many monuments that have not yet been digitised, being especially relevant those with deterioration both for digital preservation and to study means of preservation [14]. Usually, the digitization is performed only when the damage has already been done, and it is no longer possible to digitize the heritage in good condition or to compare it over time. Through the acquisition and study of the point cloud, damage in heritage can be quickly identified [15].

The aim of this work is the calculation of the volume of stone lost in the Fillaboa bridge during the floods of the recent years. The bridge was acquired using LiDAR technology and the proposed method is based on the use of the point cloud for the superposition and comparison of the two cutwaters. Cutwaters are wedge-shaped projections of bridge piers that serve to direct water flows and prevent debris from being trapped against the bridge and causing damage.

The proposed method works directly on the point cloud, without the need for modelling to other digital standards, nor the

ipAcademia
www.ipacademia.org

parameterisation of the geometric shapes composing the bridge. During the processing, the damaged area is reconstructed.

The paper is structured as follows. In Section 2, works related with the study of bridges from point clouds are collected. Section 3 is devoted to the presentation and acquisition of the case study. In Section 4, the applied method is described. In Section 5, the results are presented, and discussed. Section 6 is dedicated to the conclusion of this work.

II. RELATED WORK

This paper is focused on the creation of digital models of ancient bridges. Thus, different technologies can be used to record the as-is geometry of these assets. Nowadays, laser scanning and photogrammetry are the most common ones [16]. Through the years, photogrammetry has been used as the lead technology to study the health condition of historical assets [17–19]. As with photogrammetry, using laser scanning systems for surveying can provide geometry, relationships between elements, and other characteristics of infrastructure assets. LiDAR data can be acquired using different types of systems depending on the purpose. While aerial laser scanning (ALS) is mostly used for urban planning and for creating digital terrain models (DTM), mobile laser scanning (MLS) systems are more suitable for scanning large infrastructures like roadways. The better approach is then to use terrestrial laser scanning (TLS) systems to perform the survey of specific historical constructions [20,21], as stone bridges are. These systems usually work mounted on a stand or tripod and obtain high-resolution scans in a short period of time [in a range of minutes] [22]. A more detailed description of the use of laser scanners for surveying the terrestrial transport network can be found in [23].

concerning the automatic or semi-automatic classification of bridge point clouds [24,25]. When specifically talking about arch bridges, Walsh et al. started classifying points into different structural elements using laboratory specimens and testing real bridges [26]. Later on, Riveiro et al. developed a methodology for automatically segmenting their structural elements [27]. Concerning the inspection of masonry arch bridges, Sánchez-Rodríguez et al. showed an automatic processing method for laser scanning data in order to detect faults in their piers [28]. Once the piers were isolated from the bridge, the azimuth and elevation angles of each face were evaluated. With these values and considering the main orientation of the bridge, the possible damages affecting each pier were obtained. Other authors have also proved the validity of laser scanning for bridge inspection. Truong-Hong and Lindenbergh presented three different approaches to measure the vertical clearance of a bridge using TLS data. A review of the state of the art to this regard is presented in [29]. It is also possible to work with UAV [unmanned aerial vehicle] point clouds for the condition analysis of bridges. In [30], a method for automatically evaluating the bridge deck using said point clouds was presented.

The current trend for point cloud classification is to use algorithms that automatically predict the class of a point based on learning algorithms. Barrile et al. worked with an aerial survey of a concrete viaduct in order to apply photogrammetric reconstruction to classify the structural elements of the asset [31]. They applied image analysis techniques and used the Mask-RCNN [Region-Based Convolutional Neural Network] [32] to perform this classification. Table 1 summarizes the pros and cons of point cloud bridge processing methods.

TABLE I. SUMMARY OF STATE-OF-THE-ART WORKS FOR ARCH BRIDGES CLASSIFICATION

Reference	Processing strategy	Pros	Cons
[26]	- Sharp feature detection and segmentation	- TLS Validation in a real case study	- Concrete bridge - Use of description of predefined objects for classification - Classification only
[27]	- Dimensional analysis - Evaluation of normals (elevation and azimuth angles) Connected components	- TLS - Masonry arch bridges	- Classification only
[28]	- Evaluation of normals (elevation and azimuth angles)	- TLS - Masonry arch bridges - Classification and piers' inspection	- Focused on piers
[29]	- Review of different SoA works	- TLS - From geometric modelling to structural evaluation	- They did not develop a new methodology
[30]	- Classification: region growing Inspection: polynomial surface fitting	- Detection and deck pavement evaluation	- Concrete bridge - UAV - Imagery-based - Focused on pavement
[31]	- Deep learning (Mask-RCNN)	- Capability of successfully classifying several datasets once the model is trained	- Concrete viaduct - UAV - Photogrammetry - Classification only
Ours	- Point cloud and overlap based processing	- TLS - Applicable to any part of the bridge - Reconstruction	- Dependence of equal geometries for overlapping - No modelling

In order to use the TLS data to create a digital model of the asset scanned, a first classification of points is needed so that the elements of the bridge are grouped. There are numerous works

A new approach is the one given in this article. The main goal is to digitally fill a damaged cutwater using point cloud data only. Working with a real case study, the difference of volume between the damaged cutwater of the Fillaboa masonry arch bridge and the healthy one in the same bridge was calculated. In this way, the volume lost could be estimated, creating a digital geometric reconstruction of the damaged cutwater.

III. CASE STUDY

The bridge studied is located in the area of Fillaboa in Salvaterra de Miño, Spain. It is one of the four ancient bridges that cross the river Tea. The bridge has Roman origins in the via XX that connected Asturica Augusta with Bracara Augusta, although the current layout of the factory corresponds constructively and stylistically to the XV century, with modifications in the XVII century [33]. In medieval times, the bridge was part of the royal road between the cities of Tui and Ribadavia [34]. In the XVII century it underwent modifications and reconstructions due to the fortification of the surrounding area during the Portuguese Restoration War.

At present, the bridge has a length of 70 metres, with an approximate width of 4.5 metres. A picture of the bridge can be seen in Fig. 1. The bridge is made of granite. It has four arches, the central arch has a circular directrix, while the other three arches have a pointed shape. The piers surrounding the main arch have two cutwaters, built in the XVII century [35]. The western cutwater is the damaged one, located in the river's greatest flow. It is assumed that the damage was caused by trees washed down by the river in recent winters. The river has a water level variation of up to 10 metres, covering the bridge in its entirety in the most extreme situations.

The bridge acquisition was conducted in May 2021 with a Terrestrial Laser Scanner Faro X330 [36]. In total, six scan positions were established to obtain a global view of the case study (Fig. 2), although only positions 2 to 4 provided relevant information for the proposed method and the two cutwaters. Three acquisitions were performed at water level and three above the bridge. The eastern cutwater was easily accessible and acquirable given the low water level. The scan position 2 and 3 allowed the scanning of the two cutwater planes. The western cutwater presented more difficulty. Due to the strength of the water, closer acquisitions could not be made. Scan position 3 was used to acquire the east wall of the cutwater. Also, the west bank at river level is not accessible. Therefore, a scan position from the top of the bridge with visibility to the west wall of the cutwater was chosen (scan position 4). In addition, due to the abundant vegetation in the area surrounding the damaged cutwater and the poor visibility, drones could not be used either. The generated point cloud is shown with vegetation in Fig. 3 and filtered in Fig. 4.

Concerning the two cutwaters, the east cutwater is in perfect condition while the west cutwater is damaged. The east cutwater is larger than the west cutwater, both in height and wall length. Both cutwaters have a cutting angle of 83°. The visualisation and measurements of the cutwaters are shown in Fig. 5.

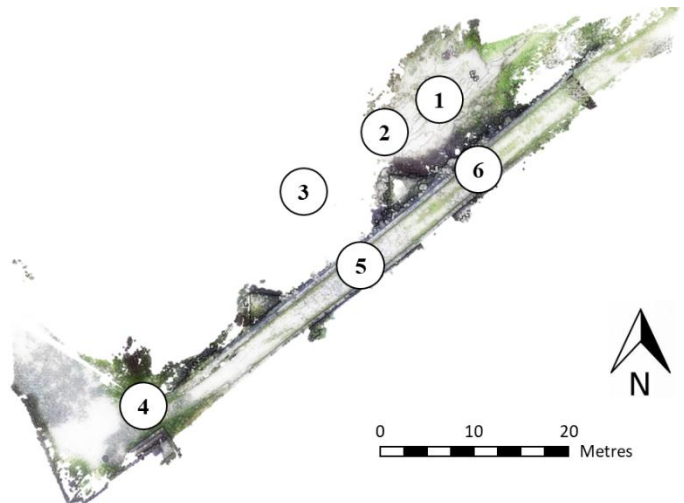Fig. 1. Photograph of the north side of the bridge (May 2021).

Fig. 2. Top view of the point cloud bridge and acquisition plan.

Fig. 3. Acquired point cloud with vegetation (north side).

Fig. 4. Point cloud of the bridge cleared of surrounding vegetation and noise.
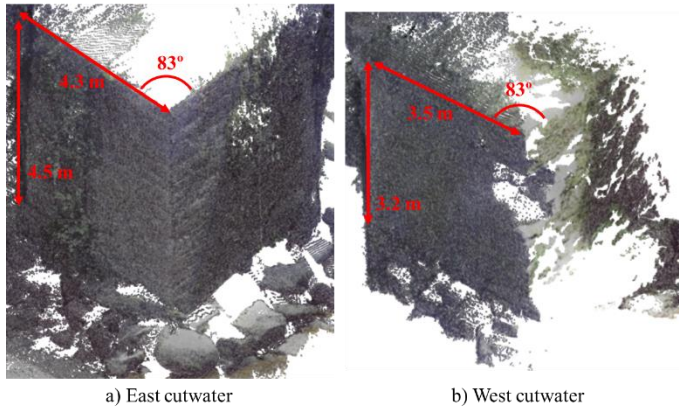

a) East cutwater   b) West cutwater

Fig. 5. Cutwaters measured in the point cloud.

a) Initial stage   b) First iteration

c) Second iteration   d) Result

☐ Data to align   ▨ Reference data

Fig. 6. Scheme of operation of the ICP algorithm in 2D data.

IV. METHOD

The proposed method is based on overlapping both cutwaters to complete the point cloud of the damaged cutwater with the complete one. For this, it is necessary that both cutwaters have the same cutting angle, which was measured at 83º for both. Moreover, the size of the entire cutwater must be sufficient to cover the damaged surface. Fortunately, the east (whole) cutwater has a height of 4.5 m, while the west (damaged) cutwater has a height of 3.2 m, of which the maximum damaged height is 1.3 m. And the wall width of the east cutwater is 4.3 m and of the west cutwater is 3.5 m.

The proposed method is divided in two main steps. First, the segmentation of both cutwaters of the bridge point cloud and the translation-fitting of the whole cutwater over the damaged one. The second is the delimitation of the damaged volume by calculating point-to-point distances between both point clouds, and the transformation of the point cloud to a 3D polygon.

A. Segmentation and alignment

Given that the measurements of the whole cutwater are sufficient to cover the damaged cutwater, both cutwaters are segmented from the point cloud bridge manually, keeping only the side walls and the inner wall of the damaged cutwater. The whole cutwater is also segmented with dimensions similar to the damaged cutwater. The aim of this segmentation is to ensure that the subsequent adjustment prioritises the walls of the cutwaters as a reference, and it is not influenced by other points, as those
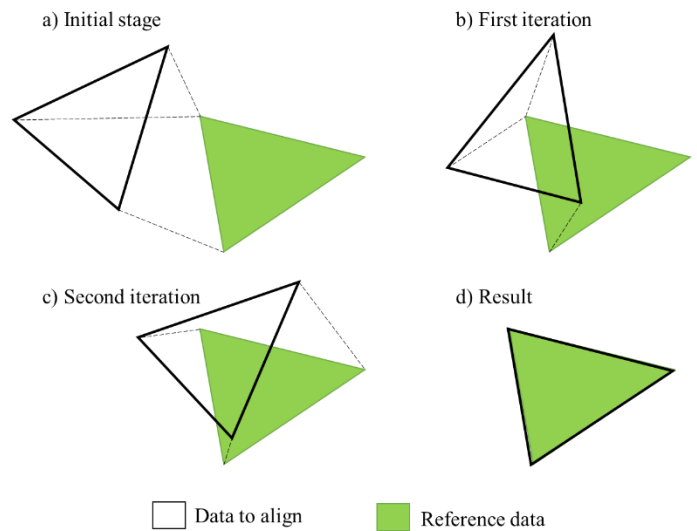
points on the rest of the bridge, thus also improving processing time.

Then, the point cloud of the whole cutwater is adjusted to the damaged cutwater by applying the Iterative Closest Point (ICP) algorithm [37]. The ICP algorithm is widely used to automatically register two point clouds of the same scene. Although there are many variants of the ICP algorithm [38–40], the simplest one is chosen in this work, since the aim is to adjust two planes intersecting at 83º. The ICP works as follows: the distance from each point of the input cloud (cutwater east) to the nearest points of the reference point cloud (cutwater west) is calculated. Then, the rotation-translation matrices minimising the distance are calculated and applied to the input cloud. The process loops from the beginning (distance estimation, matrix calculation and matrix application) until the desired error or the maximum number of iterations is reached. The point cloud of the whole cutwater is previously translated and rotated coarse manually over the damaged cutwater, so that the ICP does not reach a local minimum in the optimization. Fig. 6 shows a simplified 2D example of the ICP algorithm.

In this case, the distances of each point are calculated within a radius of 1 m to its neighbours, considering 1 m as sufficient to find points even in the centre of the damaged area. The maximum RMS (root-mean-square) error is set to 1.0E-05 m or 5 thousand iterations.

B. *Damage delineation and modelling*

Once the two point clouds are correctly aligned, a digital reconstruction of the western cutwater is obtained. In order to measure the damaged volume, it is necessary to delimit this area precisely and convert the point cloud into a closed polygon. The points enclosing the damaged volume are detected by the distance between the two point clouds. With both point clouds registered, the point-to-point distance of the cutwaters' walls is of the same order of magnitude as the point density, while the distance between points of the damaged area is larger because no points are found close to each wall.

To delimit the damaged area, the closest distance from the aligned point cloud to the reference point cloud and vice versa is calculated. As in the ICP neighbour search, the radius of the sphere around which the neighbours of each point are searched is set to 1 m. Applying this calculation to both point clouds, in the whole cutwater point cloud, the points of the surface area that would correspond to the original surface of the damaged cutwater are identified (Fig. 7.a). In the damaged cutwater point cloud, the points of the inner damage area are identified (Fig. 7.b).

To separate the damaged points, a threshold is selected from the distance calculation. Points with more than 5 cm between the two clouds are considered as areas with no data. This includes the damaged area but also some areas with noise caused by occlusions, density changes or vegetation, so a manual filtering of the area is necessary (Fig. 8).

Finally, once the point cloud encompassing the damaged volume has been created by merging the corresponding points of the clouds of both cutwaters, it is transformed into a polygon using alpha shape algorithm (41). In the 3D version, the algorithm generates spheres of α radius on whose surface three points are located. These three points are considered as the surface of the polygon if the sphere contains no other points within it. The points on the surface of the sphere are triangulated. The steps for 2D alpha shape algorithm are shown in Fig. 9.

V. RESULTS AND DISCUSSION

The conversion to polygon implies that automatic volume measurement operations can be performed. However, the alpha shape algorithm is dependent on the alpha radius, and the result can vary from an open polygon, whose volume is zero, to a convex hull shape, where shapes are simplified. It is therefore necessary to evaluate alpha with different values to find the optimum radius.

Fig. 10 shows the variation in the shape of the polygon according to the α radius, showing open triangles for α = 0.1 m and simplified triangles α = 1 m, losing precision in the measurement. Fig. 11 shows the evolution of the volume according to the α value. The optimum α value corresponds to the transition between the total or partial open polygon (low volume identified with alpha α < 0.3 m) and the polygon that is
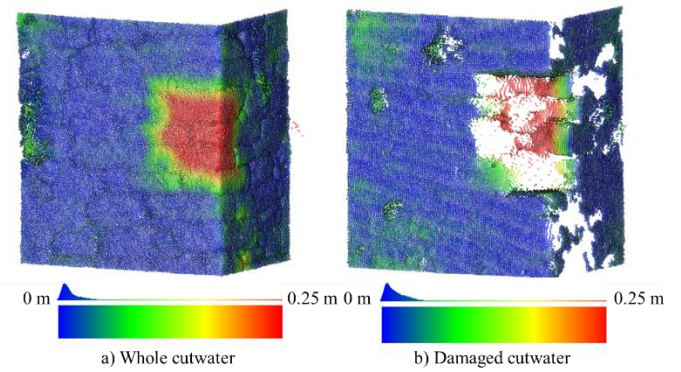

Fig. 7. Distances between aligned overlapping point clouds and identification of the damaged area.
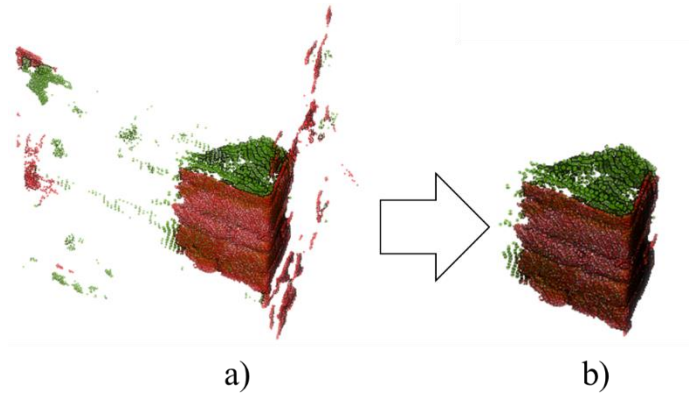

Fig. 8. Manual noise filtering: in red, the points corresponding to the whole cutwater point cloud and, in green, the points corresponding to the damaged cutwater point cloud.
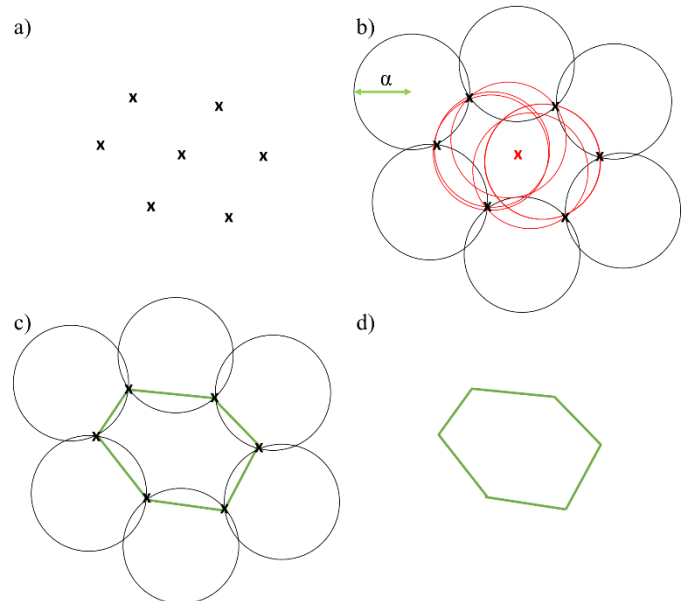

Fig. 9. Scheme of operation of the alpha shape algorithm in 2D data: a) input data; b) Generation of circumferences of α radius, circles containing a point are shown in red and those not containing a point in black; c) For empty circumferences, a line is generated connecting the input points; d) Resulting polygon

transforming into a convex hull (constant volume increments identified with α > 0.3 m). From Figure 10, the optimum alpha value is 0.3 m, which is when the polygon closes and the volume suddenly increases, and then slowly increases as it becomes more convex.

The process was implemented in Cloud Compare, except for the alpha shape algorithm and the volume calculation, which was programmed in Matlab®. Although the manual operations depend on the user's skill, each automated operation took less than 5 seconds.

Although not the main objective, by aligning the whole cutwater over the damaged cutwater and segmenting it with cloud-to-cloud distances, it was possible to generate a digital reconstruction of the area in the original state (Fig. 12). This

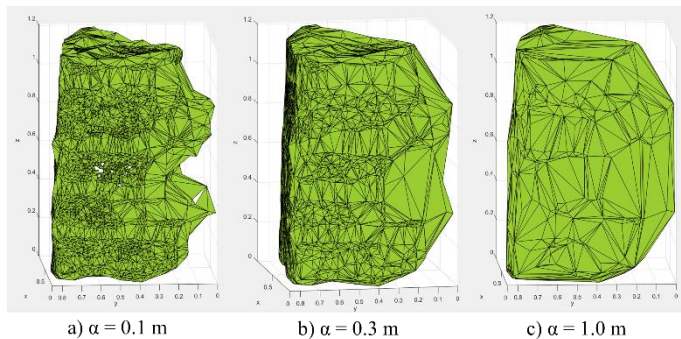a) α = 0.1 m   b) α = 0.3 m   c) α = 1.0 m

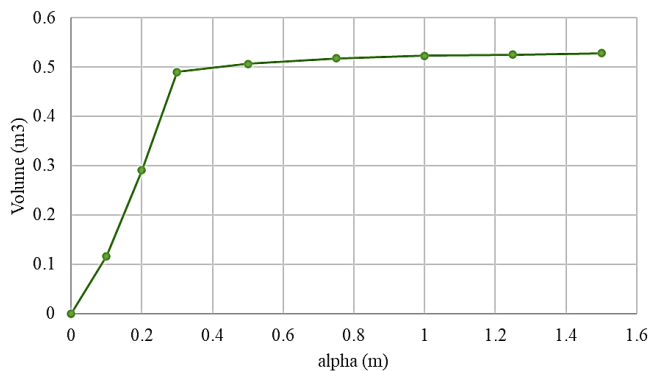Fig. 10. Polygon according to α variation.
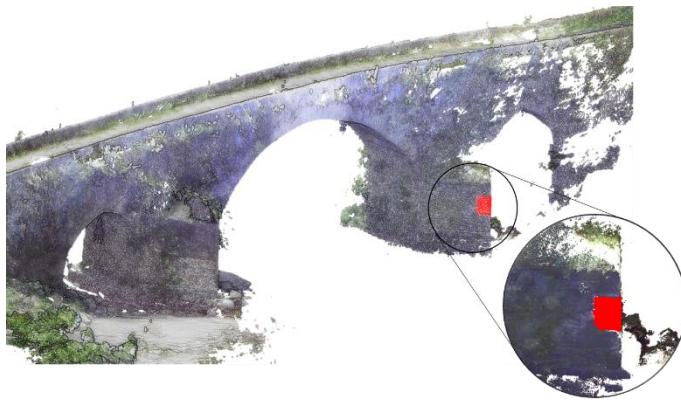

Fig. 11. Volume according to α variation.

Fig. 12. Reconstruction of the damaged area (in red).

reconstruction matches the geometry of the bridge and would enable the application of automatic segmentation algorithms of the bridge parts [27,28], not being affected by the lack of data due to the damage of the structure. Geometrically, the reconstruction matches the dimensions of the cutwater, although at masonry level, the stones do not match exactly.

There are other alternatives to achieve the result shown in this work. The most immediate would be to model the damaged cutwater as two planes to generate an undamaged model, and then to calculate the lost volume as the closed polygon formed by both planes and the envelope of the damage point cloud. However, the proposed method is more versatile because it does not depend on the modeling of the object, but only on its missing volume. Even though the method is dependent on the existence of another acquired part that allows the superposition, this in turn is an advantage because it is applicable to much more complex 3D geometric shapes, where the modeling of the whole object is not easy to achieve.

The proposed method is not free of errors, some of which have been accumulated since the data acquisition. The Faro X330 has an error of ± 2 mm for 25 m, and the registration of the scans 2 to 4 was performed with an RMS error of 60 mm. During the process, the ICP alignment produced an error of 31 mm. To the latter, the error generated by the tendency of the alpha shape algorithm to generate convex polygons must be added, although it was tried to minimise this by searching for an optimal α radius.

In addition, the difficulty of scanning and the reduced visibility to the damaged cutwater created problems that had to be solved manually, although the aim was to automate the process as much as possible. The scanning distance, and the existence of vegetation surrounding the cutwater produced occlusions and density variations in the damaged cutwater point cloud that were clearly visible in the errors in the cloud-to-cloud distance when aligning the two cutwaters. In an ideal situation, with good accessibility to the damaged cutwater, this problem would not have occurred.

As a last problem, also derived from the acquisition and the current state of the construction, much of the surface of the bridge was covered with small vegetation, although not the walls of the cutwaters. The number of points corresponding to such vegetation was low (less than 1% of the total number of points) and no effects were seen in the algorithms, beyond the noise that had to be manually segmented. However, although it is probable that in more adverse situations with more vegetation cover, surface vegetation will have a negative influence on the automatic algorithms.

VI. CONCLUSIONS

In this work, a method for modelling and estimating the volume lost in a damaged structure was presented. As a case study, the Fillaboa bridge was used, a heritage asset with high historical value. The method is based on point cloud processing, using the whole cutwater to reconstruct the damaged one and using the difference between the two point clouds to identify the damaged area.

The method allowed the damaged area to be modelled and its volume to be estimated, although manual processing was

sometimes necessary due to problems with data acquisition. The method has also proved to be computationally fast and to obtain digital geometric reconstruction of the damaged cutwater.

Future work will focus on improving the method to eliminate its dependence on manual processing. Further research will also be done on the case study, its modelling and simulation of the causes of the volume loss, as well as damage monitoring.

REFERENCES

[1] Porras-Amores C, Mazarrón FR, Cañas I, Villoria Sáez P. Terrestial laser scanning digitalization in underground constructions. Journal of Cultural Heritage. 2019;38:213–20.

[2] Popović D, Pajić V, Radović J, Govedarica M, Antonić N. Use of LiDAR technology and CityGML in the process of digitalization of cultural heritage.

[3] Pierdicca R, Paolanti M, Matrone F, Martini M, Morbidoni C, Malinverni ES, et al. Point Cloud Semantic Segmentation Using a Deep Learning Framework for Cultural Heritage. Vol. 12, Remote Sensing . 2020.

[4] Arnold E, Al-Jarrah OY, Dianati M, Fallah S, Oxtoby D, Mouzakitis A. A Survey on 3D Object Detection Methods for Autonomous Driving Applications. IEEE Transactions on Intelligent Transportation Systems. 2019;20(10):3782–95.

[5] Khanal M, Hasan M, Sterbentz N, Johnson R, Weatherly J. Accuracy Comparison of Aerial Lidar, Mobile-Terrestrial Lidar, and UAV Photogrammetric Capture Data Elevations over Different Terrain Types. Vol. 5, Infrastructures . 2020.

[6] Otero R, Lagüela S, Garrido I, Arias P. Mobile indoor mapping technologies: A review. Automation in Construction. 2020;120:103399.

[7] Wang X, Wang Y, Ma L, Yuan P, Zhang Y. Information Processing Technology in the Digital Protection of Architectural Cultural Heritage. In: 2020 International Conference on Culture-oriented Science & Technology (ICCST). 2020. p. 496–9.

[8] Griffiths D, Boehm J. A Review on Deep Learning Techniques for 3D Sensed Data Classification. Vol. 11, Remote Sensing . 2019.

[9] Malinverni ES, Pierdicca R, Paolanti M, Martini M, Morbidoni C, Matrone F, et al. Deep Learning for semantic segmentation of 3D point cloud. The International Archives of the Photogrammetry, Remote Sensing and Spatial Information Sciences. 2019;XLII-2/W15:735–42.

[10] Poux F, Hallot P, Neuville R, Billen R. SMART POINT CLOUD: DEFINITION AND REMAINING CHALLENGES. 2016.

[11] Abate D. Built-Heritage Multi-temporal Monitoring through Photogrammetry and 2D/3D Change Detection Algorithms. Studies in Conservation. 2019 Oct 3;64(7):423–34.

[12] López-Menchero Bendicho VM, Flores Gutiérrez M, Vincent ML, Grande León A. Digital Heritage and Virtual Archaeology: An Approach Through the Framework of International Recommendations BT - Mixed Reality and Gamification for Cultural Heritage. In: Ioannides M,

Magnenat-Thalmann N, Papagiannakis G, editors. Cham: Springer International Publishing; 2017. p. 3–26.

[13] Guttentag DA. Virtual reality: Applications and implications for tourism. Tourism Management. 2010;31(5):637–51.

[14] Kan T, Buyuksalih G, Enc Ozkan G, Baskaraca P. Rapid 3d Digitalization of the Cultural Heritage: a Case Study on Istanbul Suleymaniye Social Complex (KULLIYE). ISPRS - International Archives of the Photogrammetry, Remote Sensing and Spatial Information Sciences. 2019 May;4211:645–52.

[15] Balado J, Díaz-Vilariño L, Azenha M, Lourenço PB. Automatic Detection of Surface Damage in Round Brick Chimneys by Finite Plane Modelling from Terrestrial Laser Scanning Point Clouds. Case Study of Bragança Dukes' Palace, Guimarães, Portugal. International Journal of Architectural Heritage. 2021 May 23;1–15.

[16] León-Robles C, Reinoso-Gordo J, González-Quiñones J. Heritage Building Information Modeling (H-BIM) Applied to A Stone Bridge. ISPRS International Journal of Geo-Information. 2019 Mar 1;8(3):121.

[17] Franke S, Franke B, Rautenstrauch K. Strain analysis of wood components by close range photogrammetry. Materials and Structures/Materiaux et Constructions. 2007 Jan;40(1):37–46.

[18] Arias P, Armesto J, Di-Capua D, González-Drigo R, Lorenzo H, Pérez-Gracia V. Digital photogrammetry, GPR and computational analysis of structural damages in a mediaeval bridge. Engineering Failure Analysis. 2007;14(8 SPEC. ISS.):1444–57.

[19] Sonnenberg AMC, Al-Mahaidi R. Investigation of dowel shear in RC beams using photogrammetry. Magazine of Concrete Research. 2007 Nov 25;59(9):1–626.

[20] Pritchard D, Sperner J, Hoepner S, Tenschert R. Terrestrial laser scanning for heritage conservation: the Cologne Cathedral documentation project. ISPRS Annals of Photogrammetry, Remote Sensing and Spatial Information Sciences. 2017 Aug 16;IV-2/W2(2W2):213–20.

[21] Shanoer MM, Abed FM. Evaluate 3D laser point clouds registration for cultural heritage documentation. Egyptian Journal of Remote Sensing and Space Science. 2018 Dec 1;21(3):295–304.

[22] Olsen MJ, Asce M, Kuester F, Chang BJ, Asce SM, Hutchinson TC, et al. terrestrial Laser Scanned-Based Structural Damage Assessment. 2010;

[23] Soilán, Sánchez-Rodríguez, Río-Barral, Perez-Collazo, Arias, Riveiro, et al. Review of Laser Scanning Technologies and Their Applications for Road and Railway Infrastructure Monitoring. Infrastructures. 2019 Sep 20;4(4):58.

[24] Truong-Hong L, Lindenbergh R. Extracting Bridge Components from a Laser Scanning Point Cloud. In: Lecture Notes in Civil Engineering [Internet]. Springer; 2021 [cited 2021 Jun 9]. p. 721–39. Available from: https://link.springer.com/chapter/10.1007/978-3-030-51295-8_50

[25] Lu R, Brilakis I, Middleton CR. Detection of Structural Components in Point Clouds of Existing RC Bridges. Computer-Aided Civil and Infrastructure Engineering [Internet]. 2019 Mar [cited 2020 Feb 19];34(3):191–212. Available from: http://doi.wiley.com/10.1111/mice.12407

[26] Walsh SB, Borello DJ, Guldur B, Hajjar JF. Data Processing of Point Clouds for Object Detection for Structural Engineering Applications. Computer-Aided Civil and Infrastructure Engineering. 2013;28(7):495–508.

[27] Riveiro B, DeJong MJJ, Conde B. Automated processing of large point clouds for structural health monitoring of masonry arch bridges. Automation in Construction [Internet]. 2016 Dec [cited 2017 Feb 21];72:258–68. Available from: http://dx.doi.org/10.1016/j.autcon.2016.02.009

[28] Sánchez-Rodríguez A, Riveiro B, Conde B, Soilán M. Detection of structural faults in piers of masonry arch bridges through automated processing of laser scanning data. Structural Control and Health Monitoring. 2018;25(3):1–14.

[29] Truong-Hong, L., Laefer, D. F. Laser scanning for bridge inspection. In Laser Scanning 2019; 189-214.

[30] Chen S, Truong-Hong L, Laefer D, Mangina E. Automated Bridge Deck Evaluation through UAV Derived Point Cloud [Internet]. CERI-ITRN2018. 2018 Aug [cited 2021 Jun 9]. Available from: http://archive.nyu.edu/handle/2451/43478

[31] Barrile V, Candela G, Fotia A. Point cloud segmentation using image processing techniques for structural analysis. 2019;

[32] He K, Gkioxari G, Dollar P, Girshick R. Mask R-CNN. Proceedings of the IEEE International Conference on Computer Vision. 2017 Feb 1;2980–8.

[33] Freiría E. Ponte de Fillaboa [Internet]. 2013 [cited 2021 May 20]. Available from: http://patrimoniogalego.net/index.php/36706/2013/03/ponte-de-fillaboa/

[34] Ferreira Priegue EM. Los caminos medievales de Galicia. Museo Arqueolóxico Provincial; 1988. 260.

[35] Aramburu-Zabala Higuera MA, Gómez Martínez M. Juan de Herrera y su influencia: actas del simposio, Camargo, 14-17 julio 1992. Ed. Universidad de Cantabria; 1993.

[36] Frías E, Díaz-Vilariño L, Balado J, Lorenzo H. From BIM to Scan Planning and Optimization for Construction Control. Vol. 11, Remote Sensing . 2019.

[37] Li P, Wang R, Wang Y, Tao W. Evaluation of the ICP Algorithm in 3D Point Cloud Registration. IEEE Access. 2020;8:68030–48.

[38] Men H, Gebre B, Pochiraju K. Color point cloud registration with 4D ICP algorithm. In: 2011 IEEE International Conference on Robotics and Automation. 2011. p. 1511–6.

[39] Xin W, Pu J. An Improved ICP Algorithm for Point Cloud Registration. In: 2010 International Conference on Computational and Information Sciences. 2010. p. 565–8.

[40] Shi X, Liu T, Han X. Improved Iterative Closest Point(ICP) 3D point cloud registration algorithm based on point cloud filtering and adaptive fireworks for coarse registration. International Journal of Remote Sensing. 2020 Apr 17;41(8):3197–220.

[41] Edelsbrunner H, Kirkpatrick D, Seidel R. On the shape of a set of points in the plane. IEEE Transactions on Information Theory. 1983;29(4):551–9.